RESEARCH ARTICLE OPEN ACCESS

An Electrical Combi Braking System with Dual-Motor Regenerative Energy Recovery for Electric Two-Wheelers

A.Mohammed Rahil, Mohammed Aftab Vali
Dept. of Electronics & Communication Engineering, Ballari Institute of Technology and Management, Ballari, India
rahilmohammed.mrr@gmail.com
Dept. of Electronics & Communication Engineering, Ballari Institute of Technology and Management, Ballari, India
mohammedaftabvali@gmail.com

--************************----------------------------------

Abstract—

The limited driving range of electric two-wheelers remains a major barrier to their wider adoption, and India's rapidly growing electric two-wheeler market makes this limitation increasingly consequential. Conventional regenerative braking systems recover kinetic energy through the traction motor alone, so recovery efficiency falls under variable braking conditions. This paper proposes an Electrical Combi Braking System (ECBS) that combines electronic brake-force distribution with dual-motor regenerative energy recovery for electric motorcycles. The architecture retains a rear-wheel BLDC traction motor for propulsion and adds a dedicated front-wheel BLDC machine that operates solely as a generator during braking; brake-lever input is regulated by a voltage-controlled regenerative braking controller that delivers proportional braking torque while converting kinetic energy into stored electrical energy. A dual-pack battery management system distributes the recovered charge across alternating cycles to preserve battery health, and a solar-assisted auxiliary module is proposed as a supplementary charging source. An eleven-equation mathematical model of vehicle dynamics, weight-transfer-based brake-force allocation, regenerative power generation, and electrical braking torque is developed, and a MATLAB/Simulink-consistent preliminary simulation — including a parameter sensitivity analysis — is used to estimate recovered energy, battery state-of-charge recovery, and range gain. Under the stated assumptions, the simulation indicates approximately 30% greater energy recovery than a conventional single-motor system and an estimated 10-12% range improvement in urban driving, motivating hardware validation on the Donther electric-motorcycle platform.

Keywords — Electrical Combi Braking, Dual-Motor Regenerative Braking, BLDC Generator, Battery Management System, Energy Recovery, Electric Motorcycle, Weight Transfer, Sensitivity Analysis, MATLAB/Simulink Simulation.

--************************----------------------------------

I. INTRODUCTION

A. Background and Motivation

Electric two-wheelers have become an important lever for reducing urban emissions and fossil-fuel dependence, particularly in the dense, stop-and-go traffic conditions typical of Indian cities. Industry tracking indicates that electric two-wheelers reached roughly 6% penetration of total Indian two-wheeler sales by 2025, up sharply from under 1% in 2021, with the segment projected to grow at a compound annual rate well above 20% through the early 2030s as urbanization and purchase incentives continue to expand the addressable market [10]. This growth has not eliminated the practical concerns that shape day-to-day ownership: most electric scooters and motorcycles still offer a shorter realistic range than their internal-combustion counterparts, public charging infrastructure remains sparse outside major metropolitan corridors, and battery cost continues to dominate vehicle pricing [10]. Range anxiety — the rider's uncertainty about whether the remaining charge will cover the intended trip — is consistently reported as one of the strongest deterrents to adoption, especially for inter-city and daily-commute use cases where charging opportunities are limited.

Regenerative braking is one of the few range-extension techniques that requires no additional charging infrastructure, since it recovers energy that would otherwise be dissipated as heat during deceleration. In passenger cars, regenerative braking is well established and can recover a substantial fraction of urban driving energy; in electric two-wheelers, however, the technique is applied more conservatively because the traction motor is usually the only electrical machine available, and diverting it into generator mode competes with the demands of stability, drivetrain protection, and rider feel.

B. Problem Statement

Most commercial and research regenerative braking systems for electric two-wheelers recover kinetic energy solely through the traction motor [1]-[3]. Because that same machine must also deliver propulsion torque, its regenerative behaviour is a compromise: recovery efficiency falls markedly at low speed, under partial braking, and whenever the controller must prioritize ride stability over energy capture. Two-wheeler-specific studies confirm that traction-motor-only regeneration is workable but constrains how much of the available braking energy can actually be recovered, and ties the regenerative-torque envelope directly to whatever margin the propulsion drivetrain can spare [4], [5]. A second, largely separate limitation concerns how the braking force itself is divided between the front and rear wheels: because braking transfers dynamic load onto the front wheel, a front-wheel-only or poorly distributed braking strategy either wastes available front-wheel traction or risks destabilizing the rear wheel [7]. Addressing recovery efficiency and brake-force distribution together, rather than as separate problems, is the central motivation for this work.

C. Contributions of This Work

This work designs and evaluates a dual-motor regenerative braking system for electric motorcycles that separates propulsion and energy recovery into two dedicated electrical machines, combined with an electronically distributed braking strategy intended to improve both energy recuperation and braking stability. Specifically, this paper:

1) develops a dual-motor Electrical Combi Braking System (ECBS) architecture that decouples propulsion (rear BLDC motor) from regeneration (front BLDC generator);

2) formulates an eleven-equation mathematical model covering vehicle kinetic energy, weight-transfer-based front-wheel load and brake-force allocation, regenerated energy, generator power, battery state of charge, electrical braking torque, and drive-cycle-level energy and range estimation;

3) proposes a MATLAB/Simulink simulation methodology consistent with this model;

4) evaluates the closed-form model with literature-based parameters to estimate recovered energy against a conventional single-motor baseline, including a parameter sensitivity analysis; and

5) estimates the resulting effect on effective driving range under urban and highway drive cycles, and discusses the design implications and limitations of the preliminary study.

The remainder of the paper is organized as follows. Section II reviews related work across motor-integrated regeneration, two-wheeler-specific studies, brake-force distribution, and battery management. Section III describes the proposed ECBS architecture. Section IV develops the mathematical model. Section V presents the simulation methodology. Section VI reports preliminary simulation results, including a sensitivity analysis. Section VII discusses the design implications and limitations of the study, and Section VIII concludes with directions for hardware validation.

II. Literature Review

A. Motor-Integrated Regenerative Braking Control

A substantial body of work has examined how to recover braking energy through a BLDC traction motor without dedicated additional hardware. Nian et al. combine proportional-integral-derivative motor control with fuzzy-logic-based brake-force distribution to improve energy usage efficiency and extend driving distance for electric vehicles driven by a brushless DC motor [1]. Aswathi et al. similarly apply fuzzy control to regulate regenerative braking torque in a BLDC-driven electric vehicle, reporting improved recovery compared with fixed-gain control [2]. Ma and Sun take a complementary approach, proposing an energy-recovery strategy based on an ideal braking-force-distribution curve for a four-wheel-drive electric vehicle, and show that recovery gains depend strongly on how closely the actual brake-force split tracks the theoretically ideal curve [3]. Across these studies, the common thread is that smarter control of a single traction machine can meaningfully improve recovery, but the achievable ceiling is set by that machine's dual role in propulsion and regeneration.

B. Two-Wheeler-Specific Regenerative Braking Studies

Fewer studies target electric two-wheelers specifically, where lower vehicle mass, tighter packaging, and rider-perceptible braking feel impose different constraints than in four-wheeled platforms. Bobba and Rajagopal propose a compact regenerative braking scheme for a permanent-magnet BLDC-motor-driven electric two-wheeler that reshapes the inverter switching sequence to control motor-to-battery power flow without additional converters or ultracapacitors, reporting lower braking time and higher regeneration than baseline schemes [4]. More recently, Nama et al. present a modular regenerative braking circuit designed and hardware-validated for electric two-wheelers operating on hilly terrain, using state-space averaging and a Type-II current controller to track a braking-current reference across a wide range of low-speed operating conditions [5]. Both studies confirm that meaningful recovery is achievable on two-wheeler-scale hardware, but — consistent with Section II-A — both continue to route regeneration through the traction motor, leaving propulsion and energy recovery coupled through a single machine.

C. Braking-Force Distribution and Weight Transfer

Independently of how energy is recovered, motorcycle dynamics research has long established that braking transfers dynamic load from the rear wheel to the front wheel, increasing the front wheel's available traction while reducing the rear wheel's. Phalke and Agrewale analyze available braking-force distribution options for motorcycles under straight-line braking and develop a Simulink vehicle model to evaluate stability against standard test requirements, reinforcing that front-wheel braking capacity grows with deceleration while rear-wheel capacity shrinks correspondingly [7]. This dynamic-load relationship is well suited to a dual-motor regenerative architecture: because deceleration already shifts braking capacity toward the front wheel, placing the dedicated regenerative generator on the front wheel — as proposed in Section III — allocates regenerative torque to the wheel that is, by vehicle dynamics, best able to absorb it. Section IV-H develops this relationship quantitatively and uses it to justify the front-wheel regenerative-energy share assumed in the simulation of Section VI.

D. Battery Management for Regenerative Recovery

Recovered energy is only useful if it can be stored without shortening battery life. Kurkin et al. provide a comprehensive review of battery-management-system circuitry and algorithms for electric vehicles, covering cell balancing, state estimation, and charge/discharge management strategies relevant to any system that must absorb intermittent regenerative charge pulses without over-stressing individual cells [8]. Prashant et al. propose an intelligent dual-battery-system controller that uses MATLAB/Simulink-based dynamic load balancing to distribute charging and discharging across two packs, reporting improved propulsion efficiency relative to a single-pack baseline [9]. These results motivate the dual-pack, alternating-charge-cycle BMS strategy adopted in Section III-E, which is intended to spread regenerative charge pulses across two packs rather than repeatedly cycling a single pack at the point of energy recovery.

E. Summary and Research Gap

A recent comprehensive review by Szumska situates these individual contributions within the broader evolution of regenerative braking systems, tracing a shift from classical PID controllers toward model-predictive and learning-based control, and noting that in-wheel and multi-motor configurations tend to outperform single-motor architectures precisely because they allow recovery and stability objectives to be pursued with separate degrees of freedom [6]. Table I summarizes the reviewed approaches and their principal limitations.

TABLE I
COMPARISON OF EXISTING REGENERATIVE BRAKING APPROACHES

Existing Approach	Reported Limitation
Single-motor regen. braking, PID/fuzzy [1],[2]	Limited recovery during variable braking
Ideal brake-force-distribution curve [3]	Requires accurate real-time load estimation
Two-wheeler traction-motor regen. [4],[5]	Regeneration tied to propulsion drivetrain
Motorcycle brake-force distribution [7]	Addresses stability, not energy recovery
BMS circuitry / dual-pack control [8],[9]	Assumes energy source; does not address recovery hardware

Very few studies examine a dedicated secondary BLDC generator, mounted independently of the traction motor, for regenerative energy harvesting on electric two-wheelers, and none of the reviewed two-wheeler studies [4], [5] combine such a machine with an explicit, weight-transfer-informed brake-force-distribution strategy of the kind developed in [7]. This paper addresses that combined gap with a front-wheel-mounted regenerative generator that operates alongside a rear-wheel traction motor under an electronically coordinated braking strategy, decoupling regenerative-torque generation from propulsion entirely while sizing the regenerative share against the physically available front-wheel load.

III. Proposed Electrical Combi Braking Architecture

A. System Overview

The proposed ECBS comprises two independent BLDC machines, an electronic brake controller, and a dual-pack Battery Management System, as illustrated in Fig. 2:

- Rear BLDC motor: provides propulsion during normal driving.
- Front BLDC machine: operates exclusively as an electrical generator during braking.
- Electronic brake controller: converts brake-lever input into proportional regenerative braking torque.
- Dual-pack BMS: stores recovered electrical energy while protecting battery health through alternating charge cycles.

Rather than relying solely on mechanical braking, braking force is distributed electronically between the front regenerative generator and conventional hydraulic braking, which is intended to produce smoother deceleration alongside improved energy recovery. This work builds on the Donther electric-motorcycle platform (Fig. 1), which serves as the physical basis for the proposed regenerative architecture.

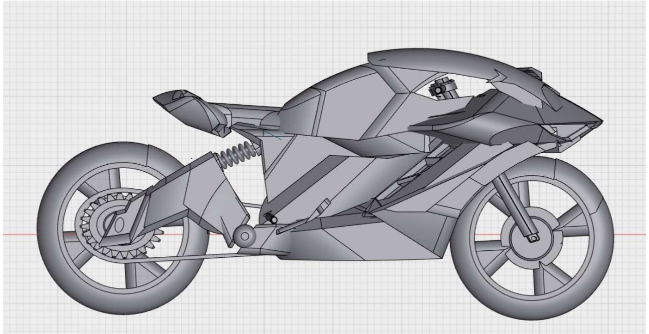

Fig. 1. CAD side-view of the Donther electric-motorcycle platform used as the physical basis for the proposed ECBS architecture.

B. Architecture Diagram

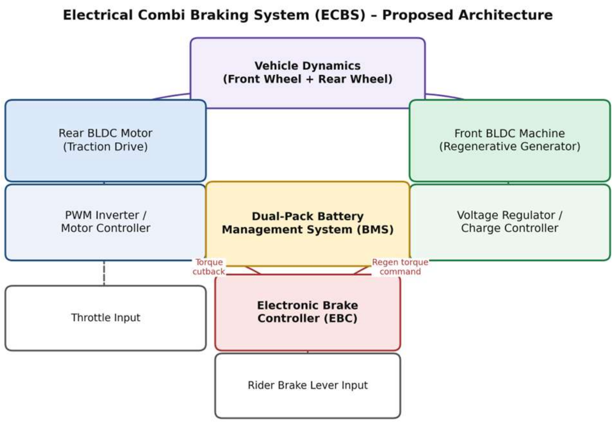

Fig. 2. Proposed Electrical Combi Braking System (ECBS) with a front-wheel regenerative generator and a rear-wheel traction motor.

C. Front BLDC Regenerative Generator

The front machine is a permanent-magnet BLDC unit sized for generator duty rather than propulsion: because it never drives the wheel under motoring torque, its winding and controller can be optimized purely for regenerative efficiency across the braking-speed range rather than for peak acceleration torque. During braking, the machine's back-electromotive-force output is rectified and regulated to the nominal bus voltage before being delivered to the BMS, consistent with the power relationship of (3) and (6). Operating the front machine exclusively as a generator, rather than switching a propulsion motor between motoring and generating modes, avoids the mode-transition delay and control complexity that motor-integrated schemes such as [1], [2], [4] must otherwise manage, at the cost of the additional mass and packaging volume of a second machine.

D. Electronic Brake Controller and Force-Distribution Strategy

The electronic brake controller (EBC) reads the rider's brake-lever position and converts it into a proportional regenerative-torque command for the front generator, while simultaneously commanding the rear traction motor to reduce driving torque, consistent with the operating-mode logic of Table II. The controller's brake-force allocation between the regenerative and hydraulic paths follows the total-force relationship of (7), with the regenerative share sized against the dynamically available front-wheel load derived in Section IV-H rather than fixed at the theoretical maximum, leaving a hydraulic margin for emergency braking and for conditions — such as a partially discharged or fully charged battery — where the BMS restricts regenerative current acceptance.

E. Dual-Pack Battery Management Strategy

The dual-pack BMS is intended to spread regenerative charge pulses across two battery packs rather than routing every braking event into a single pack, consistent with the dual-battery control strategies reviewed in Section II-D [8], [9]. In the proposed alternating-cycle strategy, one pack is designated the active discharge pack for propulsion while the second pack preferentially absorbs regenerative charge; the roles alternate once a state-of-charge threshold is crossed, so that neither pack is simultaneously subjected to high-rate discharge and high-rate regenerative charge. This is intended to reduce the cumulative cycling stress associated with repeated shallow charge/discharge events at the point of energy recovery, which the BMS literature identifies as a driver of accelerated capacity fade [8]. Each pack retains conventional protection functions — overvoltage, undervoltage, overcurrent, and thermal cutoffs — independently of the alternating-cycle logic.

F. Solar-Assisted Auxiliary Charging Module

A supplementary solar-assisted charging module is proposed as an auxiliary energy source, consistent with maximum-power-point-tracking approaches reported for two-wheeler and light-EV solar charging in the literature. The module is positioned to trickle-charge the standby pack during parking and low-speed riding, when regenerative input is intermittent or unavailable, rather than to serve as a primary charging path. Its contribution is not quantified in the simulation of Section VI, and — consistent with the scope of this paper — is presented as a design provision rather than a validated result.

G. Operating Modes

The front BLDC machine generates electrical braking torque proportional to the rider's brake input, while the rear traction motor simultaneously reduces driving torque to achieve stable deceleration. Table II summarizes the operating modes of the two machines.

TABLE II
ECBS OPERATING MODES

Mode	Rear Motor	Front Motor
Acceleration	Traction	Idle
Cruising	Traction	Standby
Light braking	Reduced torque	Low regenerative braking
Medium braking	Motor cutoff	Moderate regeneration
Emergency braking	Cutoff	Max. regeneration + hydraulic brake

H. Mechanical Integration on the Donther Platform

The rear BLDC traction motor occupies the swing-arm-mounted hub position already used for propulsion on the Donther platform shown in Fig. 1, requiring no change to the existing drivetrain layout. The front BLDC generator is packaged within the front wheel hub, in the space conventionally occupied by a disc-brake caliper mount, with the hydraulic caliper retained alongside it to preserve the mechanical brake path required by Section III-D. Routing of the generator's three-phase leads and the brake-lever sensor harness follows the existing cable routing along the front fork, so that the ECBS additions are intended to fit within the platform's existing chassis envelope rather than requiring a new frame design.

I. Novelty of the Proposed Architecture

Unlike conventional regenerative braking systems, which use only the traction motor, the proposed ECBS introduces a dedicated front-wheel BLDC generator for electrical braking. Because propulsion and regenerative torque are generated by physically separate machines, they can be controlled independently, improving brake-force distribution and allowing greater kinetic-energy recovery without significantly affecting rear-wheel traction. Placing that dedicated generator specifically on the front wheel — rather than, for example, adding a second machine to the already-driven rear wheel — further aligns the regenerative-torque path with the wheel that gains the most dynamic load during braking, as quantified in Section IV-H.

IV. MATHEMATICAL MODEL

This section develops the eleven-equation model used throughout the paper. Sections IV-A through IV-G model a single braking event; Section IV-H derives the front-wheel regenerative-share assumption from vehicle weight transfer; and Sections IV-I through IV-K extend the single-event model to a full drive cycle.

A. Vehicle Kinetic Energy

The kinetic energy of the vehicle at velocity v is given by (1), where m is the vehicle mass:

$$E_k = \frac{1}{2} m v^2 \tag{1}$$

B. Regenerated Energy

The energy recovered during a braking event, from initial velocity vi to final velocity vf, is given by (2), where ηg is the generator efficiency and ηc is the charging efficiency:

$$E_r = \eta_g \eta_c \left(\frac{1}{2} m \left(v_i^2 - v_f^2 \right) \right) \tag{2}$$

C. BLDC Generated Power

The instantaneous electrical power delivered by the front BLDC generator is:

$$P = VI \tag{3}$$

D. Battery State of Charge

The battery state of charge evolves according to (4), where C is the battery capacity and Iregen is the regenerated current:

$$SOC(t) = SOC_0 + \frac{1}{C}\int I_{regen}(t)\,dt \tag{4}$$

E. Electrical Braking Torque

The braking torque produced by the front BLDC generator is expressed as (5), where Kt is the motor torque constant and Ig is the generator current:

$$T_b = K_t I_g \tag{5}$$

F. Regenerative Electrical Power

The regenerative electrical power is given by (6), where Vg is the generated voltage and Ig is the charging current:

$$P_{regen} = V_g I_g \tag{6}$$

G. Total Braking Force

The proposed ECBS distributes the total braking force as the sum of the regenerative and hydraulic components, as given in (7):

$$F_{total} = F_{regen} + F_{hydraulic} \tag{7}$$

H. Dynamic Front-Wheel Load and Regenerative Allocation Margin

Braking transfers dynamic load from the rear wheel to the front wheel [7]. For a motorcycle with wheelbase L, centre-of-gravity height h, and static front weight fraction b/L, the front wheel's dynamic share of total weight W under a deceleration a is given by (11):

$$\frac{W_f}{W} = \frac{b}{L} + \frac{h\,a}{L\,g} \tag{11}$$

Equation (11) gives the maximum front-wheel load fraction that vehicle dynamics make available for braking at a given deceleration; it is not, by itself, the fraction of braking energy that should be routed through the front generator, since some margin must be reserved for the hydraulic path and for front-wheel-lock avoidance. The front-wheel regenerative-energy share fw used in (2) is therefore chosen as a conservative fraction of the dynamic limit given by (11); Section VI-E reports the resulting allocation ratio for the assumed vehicle geometry and compares it against the fw value used in the simulation.

I. Braking-Event Speed Profile

For a braking event initiated at speed v0 and executed at an assumed constant deceleration a, the instantaneous vehicle speed is given by (8):

$$v(t) = v_0 - a\,t \tag{8}$$

J. Cycle-Level Recovered Energy

Over a drive cycle containing n discrete braking events of the type described by (2), the total recovered energy is given by (9), assuming similar per-event conditions:

$$E_{cycle} = n \cdot E_r \tag{9}$$

K. Effective Range Gain

The corresponding effective range gain is estimated from the cycle-level recovered energy and the vehicle's nominal energy consumption per kilometre, e_avg, as given in (10):

$$\Delta R = \frac{E_{cycle}}{e_{avg}} \tag{10}$$

Equations (8)-(10) extend the single-event model of Sections IV-A to IV-G to a full drive cycle and, together with the allocation margin of (11), form the basis of the preliminary simulation study reported in Section VI.

V. MATLAB/SIMULINK METHODOLOGY

A. Block-Level Simulation Architecture

A system-level MATLAB/Simulink model is proposed to validate the mathematical formulation of Section IV prior to hardware implementation. The signal-flow structure of the model is shown in Fig. 3, and the constituent blocks are summarized in Table III. The drive-cycle and brake-profile input drives a throttle/brake control-logic block, which commands the BLDC traction-motor/inverter block during acceleration and the BLDC generator/voltage-regulator block during braking; both feed a shared vehicle-dynamics block that closes the loop back to the control logic through a vehicle-speed-feedback signal, while pack current and charge current are logged to the dual-pack battery/BMS block.

TABLE III
SIMULATION COMPONENTS

Component	Purpose
BLDC traction motor	Propulsion
Secondary BLDC generator	Regenerative energy recovery
Li-ion battery (dual-pack)	Energy storage
PWM inverter	Motor control
Voltage regulator	Charging control
Vehicle dynamics block	Load / drive-cycle model

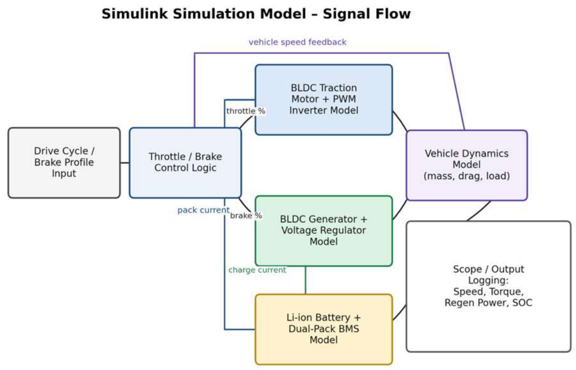

Fig. 3. Signal-flow structure of the proposed MATLAB/Simulink simulation model.

B. Closed-Form Preliminary Evaluation

Ahead of implementing the full block-level model of Fig. 3, this paper evaluates the closed-form equations of Section IV directly: for each braking condition, the vehicle speed profile of (8) is discretized, and (1)-(2) and (5)-(7) are evaluated at each time step to obtain instantaneous power, current, and torque, from which the per-event and per-cycle quantities of (9)-(10) are accumulated. This closed-form evaluation is computationally equivalent to a reduced-order version of the Fig. 3 model in which the PWM inverter and voltage regulator are represented by their steady-state efficiencies (ηg, ηc) rather than by switched, time-domain circuit models, and in which the vehicle-dynamics block is reduced to the constant-deceleration kinematics of (8). This simplification is standard practice for an early feasibility estimate, but it does not capture inverter switching transients, thermal derating, or BMS balancing dynamics; Section VI-F discusses these omissions explicitly.

C. Relationship to Planned Hardware Validation

The closed-form results of Section VI are intended to (i) confirm the internal consistency of the model of Section IV before committing engineering effort to the full Simulink build, and (ii) provide an order-of-magnitude target against which the block-level simulation and, subsequently, the hardware prototype can be compared. Because the closed-form model omits the dynamics noted in Section V-B, the block-level and hardware results are expected to differ from the figures reported here, and neither is expected to reproduce the closed-form numbers exactly.

VI. PRELIMINARY SIMULATION RESULTS AND DISCUSSION

To provide an initial, order-of-magnitude estimate ahead of hardware implementation, the closed-form model developed in Section IV (Eqs. 1-11) was evaluated numerically using the literature-based parameters listed in Table IV. These are preliminary analytical simulation results, not hardware test data; they are intended to check the internal consistency of the mathematical model and to guide the subsequent Simulink and prototype work, and should not be read as measured performance of a built system.

A. Simulation Parameters

TABLE IV
SYSTEM PARAMETERS USED IN THE PRELIMINARY SIMULATION

Parameter	Assumed Value
Vehicle + rider test mass, m	180 kg
Front-generator efficiency, ηg	0.85
Charging-path efficiency, ηc	0.90
Front-wheel braking-energy share, fw	0.55
Motor torque constant, Kt	0.50 N·m/A
Nominal bus/generator voltage, Vg	72 V
Battery pack capacity	72 V, 30 Ah (2.16 kWh)
Assumed braking deceleration, a	3.0 m/s²
Wheelbase, L (for Eq. 11)	1.35 m
CG height, h (for Eq. 11)	0.52 m
Static front weight fraction, b/L	0.50
Single-motor baseline efficiency (comparison only)	0.80

B. Braking-Event Energy Recovery

Table V reports the recovered energy, peak/average regenerative power, peak current, and peak braking torque computed from (1)-(7) for full-stop braking events at 20, 40 and 60 km/h — the planned test-matrix conditions of the original study design. Fig. 4 shows the corresponding power and torque profiles over time, and Fig. 5 compares the recovered energy against a conventional single-motor baseline computed under the same deceleration and mass assumptions, using the rear-wheel energy share and a lower single-machine generator efficiency reported for combined propulsion/regeneration machines.

TABLE V
PRELIMINARY BRAKING-EVENT SIMULATION RESULTS

Condition	Energy (Wh)	Peak Power (W)	Peak Current (A)	Peak Torque (N·m)
20 km/h → 0	0.32	1262	17.5	8.8
40 km/h → 0	1.30	2525	35.1	17.5
60 km/h → 0	2.92	3787	52.6	26.3

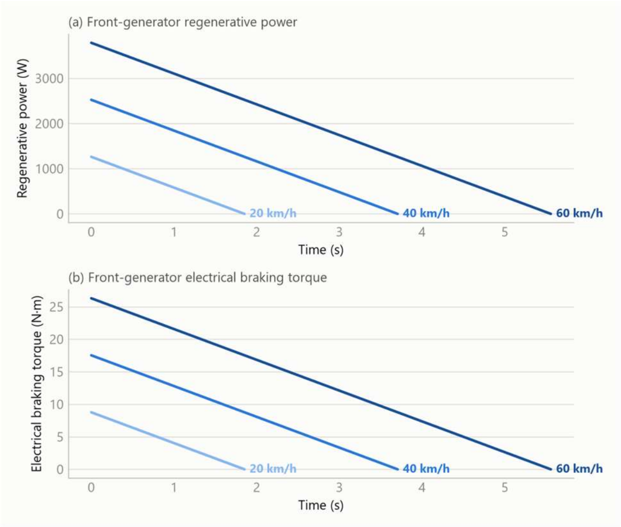

Fig. 4. Simulated front-generator regenerative power (a) and electrical braking torque (b) during 20/40/60 km/h braking events.

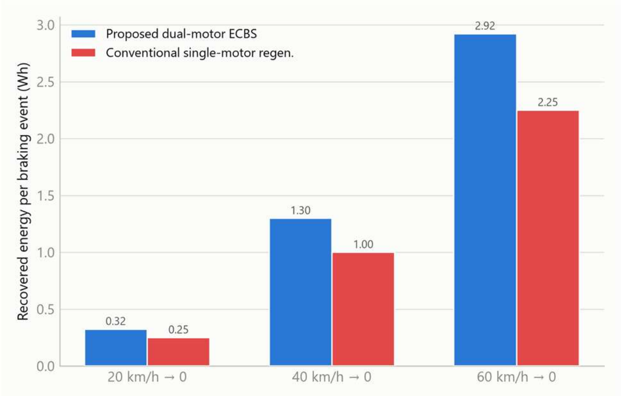

Fig. 5. Simulated recovered energy per braking event: proposed dual-motor ECBS versus a conventional single-motor regenerative-braking baseline.

Across the three braking speeds, the dual-motor ECBS model recovers approximately 30% more energy per event than the single-motor baseline under the stated assumptions (Fig. 5), consistent with directing a larger, independently controlled share of braking energy through a dedicated generator rather than sharing the traction motor between propulsion and regeneration. The improvement is constant across speeds because, in the closed-form model, both the proposed and baseline recovered-energy expressions are directly proportional to the pre-braking kinetic energy; the benefit of the dual-motor architecture in this model is therefore a fixed efficiency-and-allocation multiplier rather than a speed-dependent effect, a simplification discussed further in Section VI-F.

C. Drive-Cycle Recovery and Range Gain

Using (8)-(10), a simplified 10 km urban cycle (one braking event per 250 m from 30 km/h) and a 10 km highway cycle (one braking event per 1.5 km from 55 km/h) were evaluated; Table VI and Fig. 6 summarize the results.

TABLE VI
SIMULATED DRIVE-CYCLE RECOVERY (10 KM)

Drive Cycle	Events	Energy (Wh)	SOC Gain (%)	Range Gain (km)
Urban	40	29.2	1.35	1.17
Highway	6	14.7	0.68	0.59

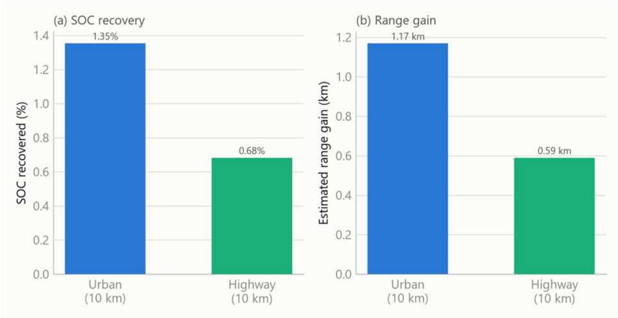

Fig. 6. Simulated SOC recovery (a) and estimated range gain (b) over 10 km urban and highway drive cycles.

The urban cycle recovers proportionally more energy and a larger range gain than the highway cycle, reflecting the higher frequency of low-speed braking events in stop-and-go traffic — consistent with the general finding in the regenerative-braking literature that recovery benefit is greatest under frequent, low-speed deceleration [6]. Scaled to a full daily commute, these per-10-km figures suggest a meaningful but modest range contribution from regenerative braking alone; the auxiliary solar-assisted charging module and the dual-pack BMS charge-cycle management are intended to compound this gain over longer trips, though quantifying that combined effect requires the hardware prototype described in Section VIII.

D. Sensitivity Analysis

Because the assumed efficiency and allocation parameters in Table IV are literature-based estimates rather than measured values, their influence on the headline recovered-energy figure was tested by varying each of ηg, ηc, and fw independently by ±10% around its baseline value and recomputing the recovered energy for the representative 40 km/h braking event. Table VII and Fig. 7 report the results.

TABLE VII
SENSITIVITY OF RECOVERED ENERGY (40 KM/H) TO ±10% PARAMETER CHANGE

Parameter	-10% (Wh)	Baseline (Wh)	+10% (Wh)
Generator eff., ηg	1.169	1.299	1.429
Charging eff., ηc	1.169	1.299	1.429
Front-wheel share, fw	1.169	1.299	1.429

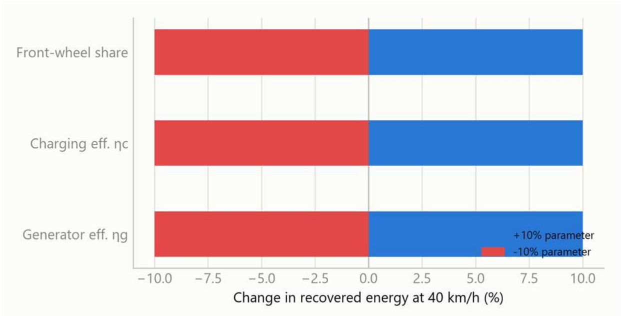

Fig. 7. Sensitivity of recovered energy at 40 km/h to a ±10% change in each model parameter, evaluated independently.

All three parameters produce an identical ±10% change in recovered energy. This is an analytical consequence of (2), in which ηg, ηc, and fw enter as a single multiplicative product rather than in a nonlinear or interacting form; the model's recovered-energy estimate is therefore exactly as sensitive to a given fractional error in any one of these three parameters as to the same fractional error in any other. Practically, this indicates that experimentally characterizing generator efficiency, charging-path efficiency, and the achieved front-wheel energy share during hardware validation is equally important across all three quantities — no single parameter can be assumed accurate at the expense of the others without proportionally biasing the recovered-energy estimate.

E. Weight-Transfer Consistency Check

Section IV-H derived the dynamic front-wheel load fraction available for braking, (11), separately from the front-wheel regenerative-energy share fw used throughout the simulation. For the assumed geometry in Table IV (wheelbase 1.35 m, CG height 0.52 m, static front fraction 0.50) and the assumed braking deceleration of 3.0 m/s², (11) gives a dynamic front-wheel load fraction of approximately 0.62. The fw value of 0.55 used in the simulation therefore corresponds to allocating approximately 89% of the dynamically available front-wheel capacity to regenerative braking, leaving roughly an 11% margin for the hydraulic path and for front-wheel-lock avoidance. This check does not validate the absolute magnitude of the recovered-energy estimates — both the geometry and the deceleration are themselves assumptions — but it confirms that the fw value used is physically conservative relative to the vehicle-dynamics limit derived independently in Section IV-H, rather than an arbitrary or optimistic figure.

F. Limitations of the Preliminary Model

Several simplifications in the closed-form evaluation should be kept in mind when interpreting Sections VI-B through VI-E. First, each braking event is modeled with a constant deceleration, whereas real braking events — and real riders — produce time-varying deceleration profiles; this affects the instantaneous power and torque profiles of Fig. 4 more than the total recovered energy, which depends only on the initial and final speeds through (2). Second, the generator and charging-path efficiencies ηg and ηc are treated as constants rather than as functions of speed, current, or battery state of charge, which is a known simplification relative to real BLDC-generator and BMS behaviour [8]. Third, the drive-cycle model of Section VI-C assumes uniform event spacing and a single representative initial speed per cycle type, rather than a measured or standardized drive cycle. Fourth, the closed-form model does not represent inverter switching losses, thermal derating, or cell-balancing dynamics, as noted in Section V-B. Each of these simplifications is a candidate refinement for the block-level Simulink model of Fig. 3 and for the hardware validation discussed in Section VIII.

VII. Discussion and Design Implications

A. Implications for Range in Urban Riding

The urban-cycle range gain of roughly 1.2 km per 10 km driven (Table VI) is modest in isolation, but electric two-wheeler range in the segment of the Indian market considered here is itself modest — commonly in the 50-80 km class [10] — so a consistent single-digit-percentage range improvement from braking energy alone is directionally useful, particularly for the tier-2/3-city and daily-commute use cases where range anxiety is most frequently reported as a barrier to adoption [10]. Because the gain scales with the number of braking events rather than distance directly, riders with more stop-and-go commutes are expected to see a proportionally larger benefit than the 10 km figures in Table VI suggest for a full working day of urban riding.

B. Safety and Stability Implications

Placing independently controllable regenerative torque on the front wheel introduces a control-design responsibility that traction-motor-only systems do not have: because the front generator can apply braking torque without any corresponding input at the rear wheel, the electronic brake controller of Section III-D must ensure that regenerative torque commands never exceed the dynamically available front-wheel traction of (11), especially on low-friction surfaces where the available traction is lower than the dry-pavement geometry assumed in Table IV. The allocation margin identified in Section VI-E — regenerative torque sized to roughly 89% of the dynamic limit — is intended to provide headroom for exactly this scenario, but the margin itself has not been validated against reduced-friction conditions and should be a specific focus of the hardware and Simulink validation phases.

C. Positioning Relative to Reviewed Literature

Relative to the motor-integrated schemes reviewed in Section II-A [1]-[3], the proposed architecture trades additional hardware (a second BLDC machine) for the ability to size and control regenerative torque independently of propulsion torque. Relative to the two-wheeler-specific studies in Section II-B [4], [5], the architecture targets the same vehicle class but removes the constraint that regeneration must share the traction motor's operating envelope. The 30% recovered-energy improvement over the single-motor baseline reported in Section VI-B is consistent in direction, though not directly comparable in magnitude, with the general observation in [6] that multi-motor and in-wheel configurations tend to outperform single-motor architectures on recovery metrics.

D. Path to Hardware Validation

The discussion above points to three concrete next steps, expanded in Section VIII: implementing the block-level Simulink model of Fig. 3 to capture the dynamics excluded from the closed-form evaluation (Section VI-F); characterizing ηg, ηc, and the achieved front-wheel energy share on the physical prototype, given their equal and substantial influence on recovered energy (Section VI-D); and validating the regenerative-torque allocation margin under reduced-friction braking conditions (Section VII-B).

VIII. Conclusion

An Electrical Combi Braking System with dual-motor regenerative energy recovery has been proposed for electric motorcycles. By separating propulsion and energy recovery into independent BLDC machines and electronically coordinating brake-force distribution between them — with the front-wheel regenerative share sized against a weight-transfer-derived dynamic-load limit — the system is intended to improve regenerative efficiency while maintaining stable braking performance. An eleven-equation mathematical model and a MATLAB/Simulink simulation methodology have been presented, and a preliminary closed-form evaluation of that model, including a parameter sensitivity analysis, indicates roughly 30% greater per-event energy recovery than a conventional single-motor baseline and a modest but consistent range benefit under urban driving. These figures depend on the literature-based parameters listed in Table IV, are equally sensitive to each of the three efficiency and allocation parameters examined in Section VI-D, and should be treated as indicative rather than conclusive. Future work includes implementing the full block-level Simulink model of Section V, fabricating a hardware prototype, experimentally characterizing the parameters identified in Section VI-D, validating the brake-force allocation margin under reduced-friction conditions, and conducting experimental validation on the Donther electric-motorcycle platform.

References

[1] X. Nian, F. Peng, and H. Zhang, "Regenerative braking system of electric vehicle driven by brushless DC motor," *IEEE Trans. Ind. Electron.*, vol. 61, no. 10, pp. 5798–5808, Oct. 2014.

[2] E. Aswathi, P. K. Prathibha, and J. R. Nair, "Regenerative braking of BLDC motor using fuzzy control for electric vehicles," *in Proc. 2nd Int. Conf. Inventive Commun. Comput. Technol. (ICICCT)*, 2018.

[3] Z. Ma and D. Sun, "Energy recovery strategy based on ideal braking force distribution for regenerative braking system of a four-wheel drive electric vehicle," *IEEE Access*, vol. 8, pp. 136234–136242, 2020.

[4] P. B. Bobba and K. R. Rajagopal, "Compact regenerative braking scheme for a PM BLDC motor driven electric two-wheeler," *in Proc. Joint Int. Conf. Power Electron., Drives Energy Syst. (PEDES) & Power India*, 2010.

[5] T. Nama, P. Mondal, P. Tripathy, R. Adda, and A. K. Gogoi, "Design, modeling and hardware implementation of regenerative braking for electric two-wheelers for hilly roads," *IEEE Access*, vol. 10, pp. 130602–130618, 2022.

[6] E. M. Szumska, "Regenerative braking systems in electric vehicles: A comprehensive review of design, control strategies, and efficiency challenges," *Energies*, vol. 18, no. 10, art. 2422, 2025.

[7] A. Phalke and M. R. B. Agrewale, "Optimal brake force distribution in motorcycle for straight-line braking," *Mater. Today Proc.*, 2nd Int. Conf. Expo. Adv. Mech. Eng., 2022.

[8] A. Kurkin, A. Chivenkov, D. Aleshin, I. Trofimov, A. Shalukho, and D. Vilkov, "Battery management system for electric vehicles: Comprehensive review of circuitry configuration and algorithms," *World Electr. Veh. J.*, vol. 16, no. 8, art. 451, 2025.

[9] Prashant, G. Verma, and R. Virmani, "An intelligent controlling in electric vehicle system with integrated DBS and BMS for sustainable solution," *Sci. Rep.*, 2026.

[10] (2026) India Electric Two-Wheeler Market Size, Share & Growth. IMARC Group. *[Online]. Available: https://www.imarcgroup.com/india-electric-two-wheeler-market*

